ELSEVIER

Applied Ocean Research 16 (1994) 101–112

0141-1187/94/$07.00

Numerical calculations of large transient water waves

T. E. Baldock & C. Swan

Department of Civil Engineering, Imperial College, London, UK, SW7 2BU

This paper concerns the description of a two-dimensional irregular sea state in which a large transient wave is generated through the constructive interference (or focusing) of the component waves. A numerical model is presented and comparisons are made with recent laboratory data. This includes measurements of the horizontal kinematics within the crest to trough region. The proposed solution is based upon a Fourier series expansion in space and time, in which the amplitude of the individual harmonics are determined by a least squares fit to the non-linear free surface boundary conditions. This approach allows for a realistic mix of free waves (with differing phase velocities) and their associated bound waves. The solution, which is not assumed to be either locally or globally steady, can be used to predict the kinematics beneath a recorded (or predicted) water surface elevation. The numerical results are in excellent agreement with the laboratory data, and the solution is robust in the sense that convergence is always achieved from simple initial conditions. The proposed model is not computationally intensive and may thus be suitable for design calculations.

1 INTRODUCTION

The design calculations appropriate to the safety and serviceability of any offshore structure are dependent upon a reliable estimate of both the maximum water surface elevation and the underlying kinematics. For example, in the case of a fixed jacket structure, the water surface elevation is required for air gap calculations, while the underlying kinematics will determine both the local forces on individual members and the global values of the base shear and the overturning moment. To simplify these calculations it has become common practice to assume that the largest ocean waves can either be modelled by an 'equivalent' regular wave or a steady state solution (Dean[1]) in which the gross characteristics of the wave are identified by a long time series simulation of a random sea state.

However, recent field data (Rozario *et al.*[2]; Sand *et al.*[3]) have shown that the largest ocean waves do not usually arise as part of a regular wave train, but occur as individual events which rapidly disperse in both space and time. Indeed, the formation of the largest waves is believed to be associated with the focusing of wave energy whereby the phasing of the individual wave components is such that constructive interference occurs at one point in space and time. The occurrence of these events has been considered by Tromans *et al.*[4] Unfortunately, this so-called 'Newave' solution is only valid to a first order of wave steepness and therefore neglects the non-linear wave–wave interactions. Indeed, comparisons with both recent laboratory data (Baldock *et al.*[5]) and field data collected from the Tern platform in the northern North Sea (Rozario *et al.*[2]; Tromans *et al.*[6]) suggest that a linear solution will under-estimate both the maximum water surface elevation and the near surface kinematics.

The present paper will address these points and will present the results of a numerical formulation based upon a double Fourier series expansion first adopted by Lambrakos.[7] Section 2 commences with a brief review of the existing kinematic models. The numerical formulation is outlined in Section 3 and comparisons are made in Section 4 with both the existing solutions and the experimental data presented by Baldock *et al.*[5] Finally, some conclusions are proposed in Section 5 and the practical implications of the numerical results briefly outlined.

2 PREVIOUS WORK

The complexity of a large transient wave arises because the fluid motion is both highly non-linear, unsteady and irregular. To overcome these difficulties the existing design solutions adopt one of two approximations. In the first case they may neglect the time dependence of the wave motion and apply a regular or steady state solution. Alternatively, the non-linearity may be neglected and a linear random wave solution applied. This latter approach is often combined with an empirical modification (or 'stretching') of the kinematics within the crest to trough region.

In the first case one could seek to define an appropriate wave height (H) and wave period (T), so that a higher order Stokes' solution (Fenton[8]) may be applied to an 'equivalent' regular wave. Unfortunately, previous researchers (including Kinsman[9]) have shown that the predicted water surface elevation may differ considerably from a measured record. To address this difficulty the non-linear boundary conditions may be satisfied numerically along a measured surface profile. This approach was first proposed by Dean[1] for steady waves with irregular surface profiles. Although these solutions are both non-linear, the transient nature of a large focused wave is neglected, and significant errors may therefore result.

The second approach incorporates the time dependence by superimposing a large number of small amplitude waves. If the wave heights (H_i), wave frequencies (ω_i) and wave numbers (k_i) of the freely propagating small amplitude waves are known, a linear random wave model will provide a first estimate of the time dependent solution. However, this approach neglects the non-linearity of the flow field, and in particular the wave–wave interactions first proposed by Longuet-Higgins and Stewart.[10] Baldock *et al.*[5] have considered these interactions in the context of a focused wave group such that the total second order interaction is given by the sum of the interactions arising from each potential 'pair' of wave components. Although this solution provides an improved description of a focused wave group, a comparison with recent laboratory data (Baldock *et al.*[5]) suggests that the higher order interactions (O. $\{a^3k^3\}$ and above) cannot be neglected. This is consistent with the numerical calculations presented by Longuet-Higgins[11] in which he showed that the wave–wave interactions become highly non-linear when the steepness of the long wave increases. These results are also in agreement with the arguments outlined by Dean[12] in which he suggested that the non-linear wave–wave interactions provide a possible mechanism for the formation of the largest or 'freak' wave events.

The second order solution outlined by Longuet-Higgins and Stewart[10] concerns the interaction of freely propagating wave trains. Unfortunately, it is difficult to identify these waves from a recorded time history of the water surface elevation. A Fourier transform of a recorded profile will provide an estimate of the power spectrum from which the amplitude of the wave components may be inferred. However, it is not possible to distinguish (with any degree of certainty) which wave components are free, and which components arise from the non-linear interactions and may therefore be bound (both spatially and temporally) to the interacting free waves. To address this point Petti[13] has proposed a method to distinguish the first and second order terms within a measured time series. Unfortunately, this approach is not capable of isolating the higher order terms. Errors of this type have led to the over-prediction of the kinematics within the crests of large random waves. In essence these problems arise because firstly, a linear random wave model does not allow the individual wave components to ride over one another, and secondly, it does not differentiate between the free waves and the bound waves which will have a significantly different dispersion relationship. As a result, the velocities associated with the high frequency waves are extrapolated to the crests of the longer waves and an over-prediction results. This effect is often referred to as high frequency contamination, and has been considered by a number of authors including Forristall[14] and Sobey.[15]

To overcome this difficulty a number of empirical solutions have been proposed. These are based upon both laboratory and field data, and seek to reduce the near surface kinematics in an attempt to compensate for the occurrence of high frequency contamination. The first and perhaps the most common method was proposed by Wheeler,[16] although a number of similar approaches have been presented by Chakrabarti,[17] Rodenbusch and Forristall,[18] Lo and Dean[19] and Gudmestad and Connor.[20] These solutions are widely used in design calculations. However, they do not satisfy the governing field equations and recent work by Gudmestad and Haver[21] concludes that they are sensitive to both the degree of non-linearity and the upper limit of the spectral analysis. In light of these, and other difficulties, the authors of this paper would not expect these empirical solutions to provide a good description of the kinematics associated with a highly non-linear focused wave group.

In addition to the design solutions discussed above a number of advanced numerical models have also been used to describe a non-linear irregular wave train. For example, Dold and Peregrine[22] describe a boundary element method which allows the investigation of the non-linear wave–wave interactions in both the spatial and the temporal domains. However, this solution requires a spatial description of the wave group. Although this information is not easily obtained from a time history of the water surface elevation at one spatial location, Skyner *et al.*[23] have shown that this numerical formulation is in good agreement with laboratory measurements of breaking waves. Sobey[24] provides an alternative approach based on a local Fourier approximation which is (in some respects) similar to the polynomial approximation proposed by Fenton.[25] In the local Fourier solution the recorded water surface elevation is sub-divided into a large number of small 'windows', within which the solution is assumed to be locally steady. This approach has been shown to be in good agreement with higher order steady state solutions, but has not thus far been used to predict the kinematics beneath a highly transient focused wave group. The present paper will consider an alternative solution based upon a method first proposed by Lambrakos.[7] The advantage of this approach is that the computational requirements are not excessive, and since the solution is based upon a time history of the water surface elevation, it may represent an effective design tool.

3 NUMERICAL MODELLING

The numerical model described within this section is based upon a double Fourier series expansion first adopted by Lambrakos.[7] This approach provides a description of a non-linear unsteady wave train in both the spatial and the temporal domains. To achieve these results using a Fourier series one must assume that there is some fundamental (or characteristic) wave period. This implies that both the water surface elevation and the underlying kinematics are periodic over some large spatial/temporal domain. However, within this region the solution may deform in both space and time. Although this periodic constraint is rarely (if ever) valid, the numerical results suggest that the solution is not strongly dependent upon this assumption provided that the fundamental period is sufficiently large. Indeed, the solution is shown to provide a good description of a large transient wave generated by the focusing of wave energy.

Although the proposed model is similar to that described by Lambrakos,[7] a comparison with recent laboratory data (Section 4) has led to a number of significant changes. In particular, a weighting function is introduced so that the time history of the water surface elevation at one spatial location is sufficient to define the flow field in the vicinity of the measuring location.

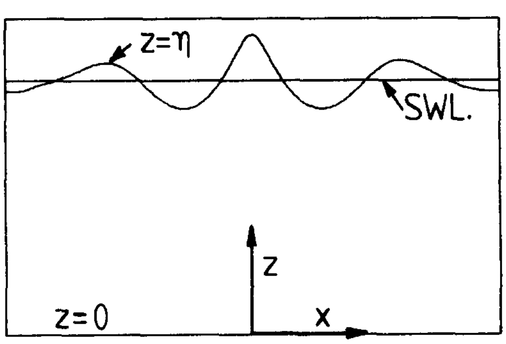

Fig. 1. Co-ordinate axes.

Governing equations

If a uni-directional irregular wave train is propagating in an inviscid, homogeneous and incompressible fluid of constant depth, the fluid motion may be assumed irrotational and the conservation of mass gives:

$$\frac{\partial^2\phi}{\partial x^2}+\frac{\partial^2\phi}{\partial z^2}=0 \tag{1}$$

where the velocity potential, ϕ, is defined so that the velocity components (u, v) in the (x, z) directions are given by:

$$u=-\frac{\partial\phi}{\partial x}, \qquad v=-\frac{\partial\phi}{\partial z} \tag{2}$$

A sketch showing the orientation of the co-ordinate axes is given in Fig. 1. Equation (1) represents the governing field equation which is subject to the usual boundary conditions.

(a) If the bed is impermeable the vertical velocity must reduce to zero at $z = 0$:

$$-\frac{\partial\phi}{\partial z}=0 \quad \text{at} \quad z=0 \tag{3}$$

(b) The kinematic free surface boundary condition dictates that the water surface should be a streamline:

$$\frac{\partial\eta}{\partial t}-\frac{\partial\phi}{\partial x}\frac{\partial\eta}{\partial x}=-\frac{\partial\phi}{\partial z} \quad \text{on} \quad z=\eta \tag{4}$$

where $\eta(x, t)$ is the water surface elevation measured in a stationary frame of reference.

(c) The dynamic free surface boundary condition requires the pressure to be constant on the water surface. Applying the unsteady Bernoulli equation we obtain:

$$\eta-\frac{1}{g}\frac{\partial\phi}{\partial t}+\frac{1}{2g}\left(\left[\frac{\partial\phi}{\partial x}\right]^2+\left[\frac{\partial\phi}{\partial z}\right]^2\right)=Q \quad \text{on} \quad z=\eta \tag{5}$$

where Q is the Bernoulli constant.

Fourier solution

The velocity potential adopted by Lambrakos[7] represents a Fourier series expansion in the spatial and the temporal domains:

$$\phi(x,z,t)=\sum_{m=1}^{M}\sum_{n=1}^{N}-\cosh(k_n z)(A_{mn}\cos(k_n x-\omega_m t) + B_{mn}\sin(k_n x-\omega_m t)) \tag{6}$$

where A_{mn}, B_{mn}, ω_m and k_n are constants for a given solution. In accordance with our previous discussion a Fourier series solution of this type requires the definition of a fundamental period T_1. If this is taken as the time

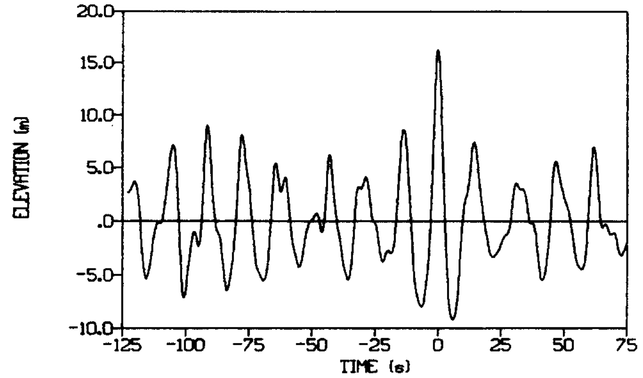

Fig. 2. A large ocean wave. Measurements taken from the Tern Platform (Northern North Sea) and provided by Shell Exploration & Production (UK) Limited.

span of a chosen segment of the surface record, the first (or fundamental) harmonic will have a frequency $\omega_1 = 2\pi/T_1$. The corresponding value for the wave length L_1, and therefore the wave number k_1 $(2\pi/L_1)$, is calculated using the minimisation procedure discussed below. In the present study we are primarily concerned with the formation of a large transient wave, and consequently the most appropriate segment of the surface record is that which contains the focused wave crest. For example, Fig. 2 shows the water surface elevation recorded in January 1992 at the Tern platform located in the northern North Sea (Rozario *et al.*[2]). It is data of this type which we will attempt to model using the potential function given in eqn (6). In all cases the value of T_1 was chosen so that it was significantly larger than the maximum period of the component waves. Having identified a fundamental period, the remaining Fourier components are defined by:

$$\omega_m = m\omega_1, \qquad k_n = nk_1 \tag{7}$$

where m and n are integers having maximum values of M and N, respectively.

The potential function given in eqn (6) allows the wave group to deform in both space and time. Furthermore, the combination of wave frequencies (ω_m) and wave numbers (k_n) introduces wave components having different phase velocities (ω_m/k_n). This is in marked contrast to the steady state solutions (Chappelear,[26] Dean[1] and Chaplin[27]) where all the harmonic components have the same phase velocity. Table 1 concerns the phase velocity (measured relative

Table 1. Phase velocity relative to the fundamental

	ω_1	ω_2	ω_3	ω_4	ω_5	ω_6
k_1	1	2	3	4	5	6
k_2	1/2	**1**	3/2	**2**	5/2	**3**
k_3	1/3	2/3	**1**	4/3	5/3	**2**
k_4	1/4	**1/2**	3/4	**1**	5/4	**3/2**
k_5	1/5	2/5	3/5	4/5	**1**	6/5
k_6	1/6	**1/3**	**1/2**	**2/3**	5/6	**1**

to the fundamental) of the first 36 wave components ($M = 6$, $N = 6$). These values emphasise the range of phase velocities and demonstrate that the proposed solution represents a combination of free waves and their associated bound waves (indicated in bold type). Although the wave components described in Table 1 are defined by the appropriate Fourier modes, the amplitudes of the individual harmonics (A_{mn}, B_{mn}) are dependent upon the boundary conditions. As a result, not all the components described in Table 1 will be relevant, and the final solution will converge to the appropriate mix of free waves and bound waves which minimise the errors in the boundary conditions (see below). In the present study we will only consider uni-directional waves. This is consistent with the experimental observations (Section 4) in which the reflection of wave energy at the downstream end of the wave flume was virtually eliminated (< 2% of the incident wave height) by the installation of an effective passive absorber. However, the inclusion of negative wave numbers in eqn (7) would allow the numerical scheme to consider the interaction of waves travelling in opposite directions.

Computational procedure

Since the Fourier series expansion given in eqn (6) satisfies both the governing eqn (1) and the bottom boundary condition (3), the unknown coefficients (A_{mn}, B_{mn}) must be defined to minimise the error in the non-linear free surface boundary conditions. If $E_{\mathrm{K}ij}$ represents the error in the kinematic free surface boundary condition at (x_j, t_i) and $E_{\mathrm{D}ij}$ is the equivalent error in the dynamic free surface boundary condition, eqns (4) and (5) respectively give:

$$E_{\mathrm{K}ij} = \left(\frac{\partial\eta}{\partial t} - \frac{\partial\phi}{\partial x}\frac{\partial\eta}{\partial x} + \frac{\partial\phi}{\partial z}\right) \quad \text{on} \quad z = \eta(x_j, t_i) \tag{8}$$

$$E_{\mathrm{D}ij} = \left(\eta - \frac{1}{g}\frac{\partial\phi}{\partial t} + \frac{1}{2g}\left[\left(\frac{\partial\phi}{\partial x}\right)^2 + \left(\frac{\partial\phi}{\partial z}\right)^2\right] - Q\right) \quad \text{on} \quad z = \eta(x_j, t_i) \tag{9}$$

After non-dimensionalising with respect to the fundamental frequency (ω_1), the total error in the non-linear free surface boundary conditions (E_{T}) is:

$$E_{\mathrm{T}} = \sum_{i=1}^{I}\sum_{j=1}^{J}\left[\left(E_{\mathrm{D}ij}\frac{\omega_1^2}{g}\right)^2 + \left(E_{\mathrm{K}ij}\frac{\omega_1}{g}\right)^2\right] \tag{10}$$

where I and J are of equal magnitude and denote the number of temporal and spatial locations at which the boundary conditions are evaluated.

If the proposed solution includes M frequency components each with N wave numbers (where typically $M = N$) a total of $2MN$ Fourier coefficients are created. Adding to this the wave number of the fundamental harmonic (k_1) and the Bernoulli constant (Q) gives a total of $2(MN+1)$ unknowns. To solve these parameters by minimising the errors in the free surface boundary conditions requires some initial (or trial) values from which an iterative solution will converge. In the present case a first order wave theory was found to be sufficient to provide both an initial estimate for k_1 and a single velocity potential coefficient (i.e. A_{mn} or B_{mn}) describing the dominant harmonic in the measured water surface elevation. All the remaining coefficients were initially set to zero.

With these initial conditions a first estimate of the boundary condition error E_T may be obtained from eqn (10). If E_T is quasi-linearised by expanding the unknown parameters $X(p)$, where $1 \le p \le 2[MN+1]$, in a first order Taylor series about the previous iteration, successive values of E_T are given by:

$$E_T^{q+1} = E_T^q + \sum_{p=1}^{2(MN+1)} \frac{\partial E_T^q}{\partial X(p)} X'(p) \tag{11}$$

where q is merely a counter corresponding to the number of iterations, and the $X'(p)$ represent small changes in the unknown parameters. If E_T^{q+1} is minimised with respect to the unknowns ($X(p)$), $2(MN+1)$ equations result:

$$\frac{\partial E_T^{q+1}}{\partial X(1)} = 0, \quad \frac{\partial E_T^{q+1}}{\partial X(2)} = 0, \ldots$$
$$\ldots, \quad \frac{\partial E_T^{q+1}}{\partial X(2MN+2)} = 0 \tag{12}$$

from which the values of $X'(p)$ may be obtained by standard matrix decomposition and back substitution methods (Press *et al.*[28]). After each iteration the new value of each unknown parameter is

$$X(p)^{q+1} = X(p)^q + \lambda X'(p) \tag{13}$$

where λ represents a damping factor. This reduces the change in the unknown parameters between successive iterations and therefore improves the stability of the iterative scheme. In the present study $\lambda = 0{\cdot}6$ was sufficient to achieve convergence in all cases.

If the present scheme is to be based upon the recorded water surface elevation at one spatial location (i.e. $\eta(t)$ at $x = x_r$), the time history of the water surface elevation at all other spatial locations ($x \ne x_r$) must be determined within the iterative procedure. If $\eta(x_j, t_i)^q$ corresponds to the water surface elevation after q iterations at $x = x_j$ and $t = t_i$, the dynamic free surface boundary condition gives the surface elevation at the next iteration as:

$$\eta(x_j, t_i)^{q+1} = \left(\frac{1}{g}\frac{\partial \phi^q}{\partial t} - \frac{1}{2g}\left(\left(\frac{\partial \phi^q}{\partial x}\right)^2 + \left(\frac{\partial \phi^q}{\partial z}\right)^2 \right) + Q^q \right)_{z=\eta^q} \tag{14}$$

Using this approach the dynamic free surface boundary condition is not satisfied exactly, but the error E_{Dij} reduces to zero as $\eta^{q+1} - \eta^q \to 0$ within the iterative procedure. This method is different to that adopted by Lambrakos.[7] In his solution the dynamic free surface boundary conditions appears to be solved exactly to give $\eta(x_j, t_i)$ at each iteration. As a result, the only contribution to E_T at all points $x \ne x_r$ comes from the kinematic free surface boundary condition. Neither E_{Dij} or (more importantly) $\partial E_{Dij}/\partial X(p)$ were calculated within his iterative procedure. This approach has also been considered in the present study and calculations have shown that it significantly increases the number of iterations required for convergence.

Although the solution outlined above is (potentially) capable of describing a large transient wave, a preliminary comparison with the experimental data (Section 4) highlighted an important limitation. This arises because the sum of the errors ($E_{Dij} + E_{Kij}$) at all points in space and time does not adequately take into account the input to the numerical model which occurs at one spatial location. In essence, the least squares fit to the boundary conditions is dominated by the large number of spatial locations at which measured data is not provided. The solution may therefore under-estimate the amplitude of the surface record at $x = x_r$ in an attempt to minimise E_{Kij} at $x \ne x_r$. As a result, the numerical model provides a poor fit to the measured

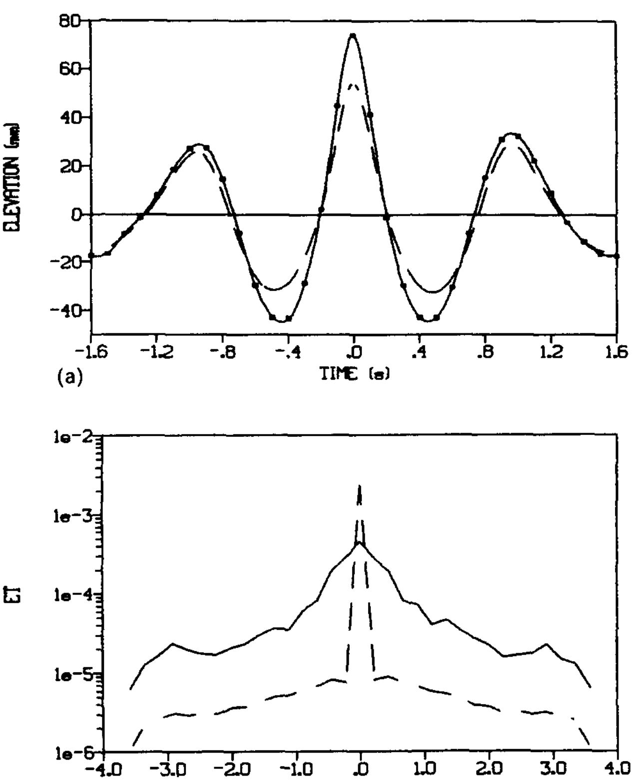

Fig. 3. (a) Predictions of the water surface elevation, $\eta(t)$, (b) boundary condition error, E_T. Measured data (■■■); weighting factor: (- - - -) $F = 1$; —— $F = 50$.

Table 2. Test conditions for experimental data (after Baldock *et al.*[5])

Case	Period range	Input amplitude, A (mm)
B2	$0{\cdot}6 \leq T \leq 1{\cdot}4$	38
B3	$0{\cdot}6 \leq T \leq 1{\cdot}4$	55
D2	$0{\cdot}8 \leq T \leq 1{\cdot}2$	38
D3	$0{\cdot}8 \leq T \leq 1{\cdot}2$	55

water surface elevation and under-estimates the non-linearity of the sea state. To overcome this difficulty a weighting function (F_j) is introduced within eqn (10). Calculations have shown that this parameter is of considerable importance since the input data (at $x = x_r$) provides the only link between the numerical formulation and the physical problem. If the predicted water surface elevation does not provide a good fit to the input data at $x = x_r$, the spatial evolution of the wave group cannot be satisfactorily modelled. The total error E_T thus becomes:

$$E_T = \sum_{i=1}^{I}\sum_{j=1}^{J}\left[\left(F_j E_{Dij}\frac{\omega_1^2}{g}\right)^2 + \left(E_{Kij}\frac{\omega_1}{g}\right)^2\right] \qquad (15)$$

where $F_j \geq 1$ at $x = x_r$ and $F_j = 1$ at $x \neq x_r$. The value of $F_j(x = x_r)$ is dependent upon the non-linearity of the sea state. In practice it may be determined iteratively by increasing its value until there is no change in the predicted water surface elevation. However, in the present study $F_j(x = x_r) = 50$ was found to be appropriate for all cases. The influence of this weighting function is clearly identified in Fig. 3(a) and 3(b). Figure 3(a) concerns the free surface elevation at $x = x_r$ and compares the experimental data (case D3) provided by Baldock *et al.*[5] with two runs of the numerical model. In the first case $F_j(x = x_r) = 1$, while in the second $F_j(x = x_r) = 50$. In all other respects the numerical simulations were identical. Figure 3(b) concerns the same case and presents the total error in the free surface boundary conditions at each spatial location. With $F_j(x = x_r) = 1$ the fit to the measured data is poor, but the total error E_T is a minimum because the solution under-estimates the non-linearity of the wave group. However, at $x = x_r$ there is a large discontinuity in the total error since the boundary condition errors at this location are based upon the measured water surface elevation. With $F_j(x = x_r) = 50$ the numerical solution adequately reflects the non-linearity of the measured sea state, and although the errors are larger at $x \neq x_r$ they are more realistically distributed across the spatial domain.

Finally, the resolution of the numerical scheme (in

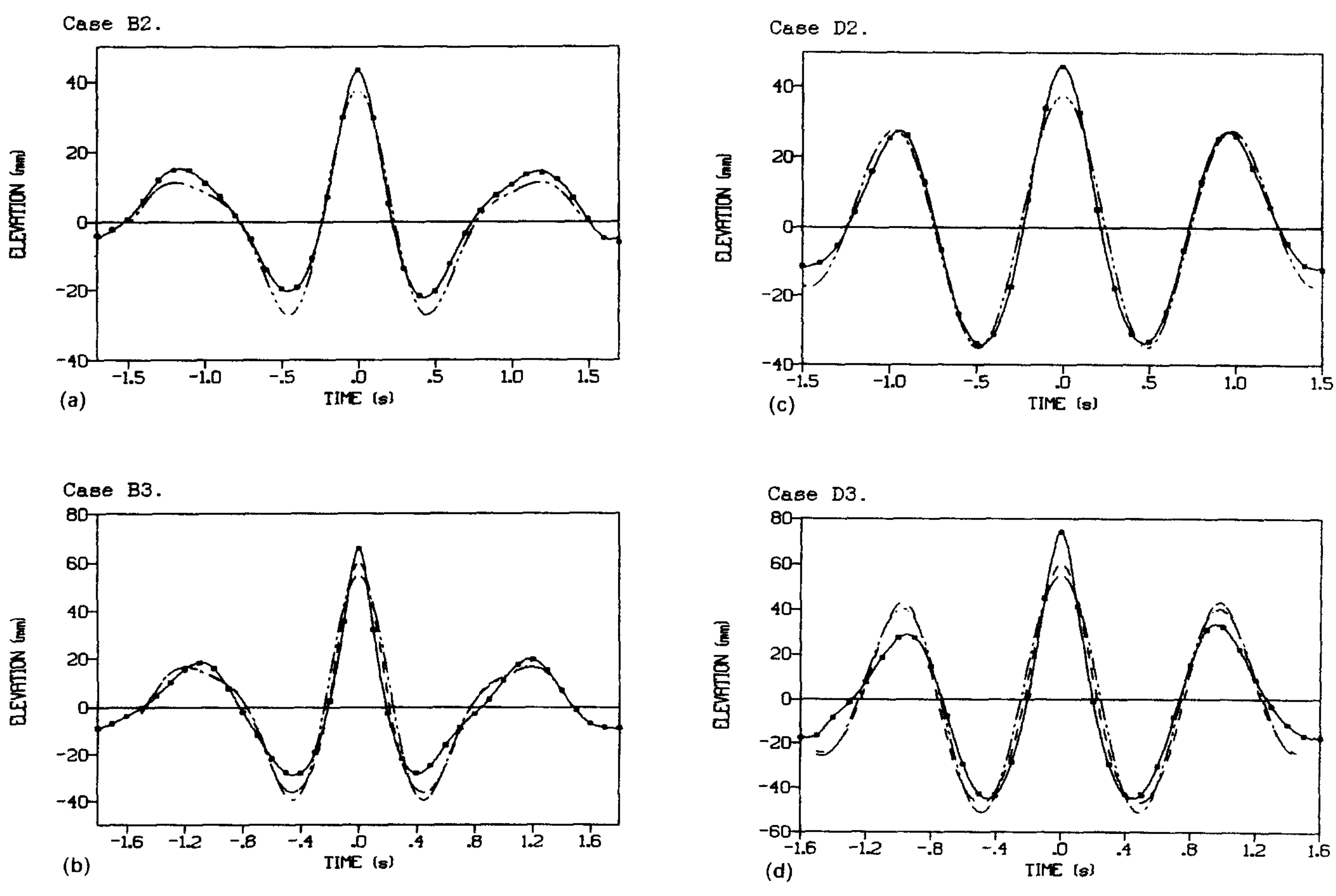

Fig. 4. Surface elevation, $\eta(t)$: (· · ·) Measured data; (- — -) linear solution; (- - - -) 2nd order solution; (——) numerical model ((a) & (b) $M = N = 18$, $F = 50$; (c) & (d) $M = N = 15$, $F = 50$).

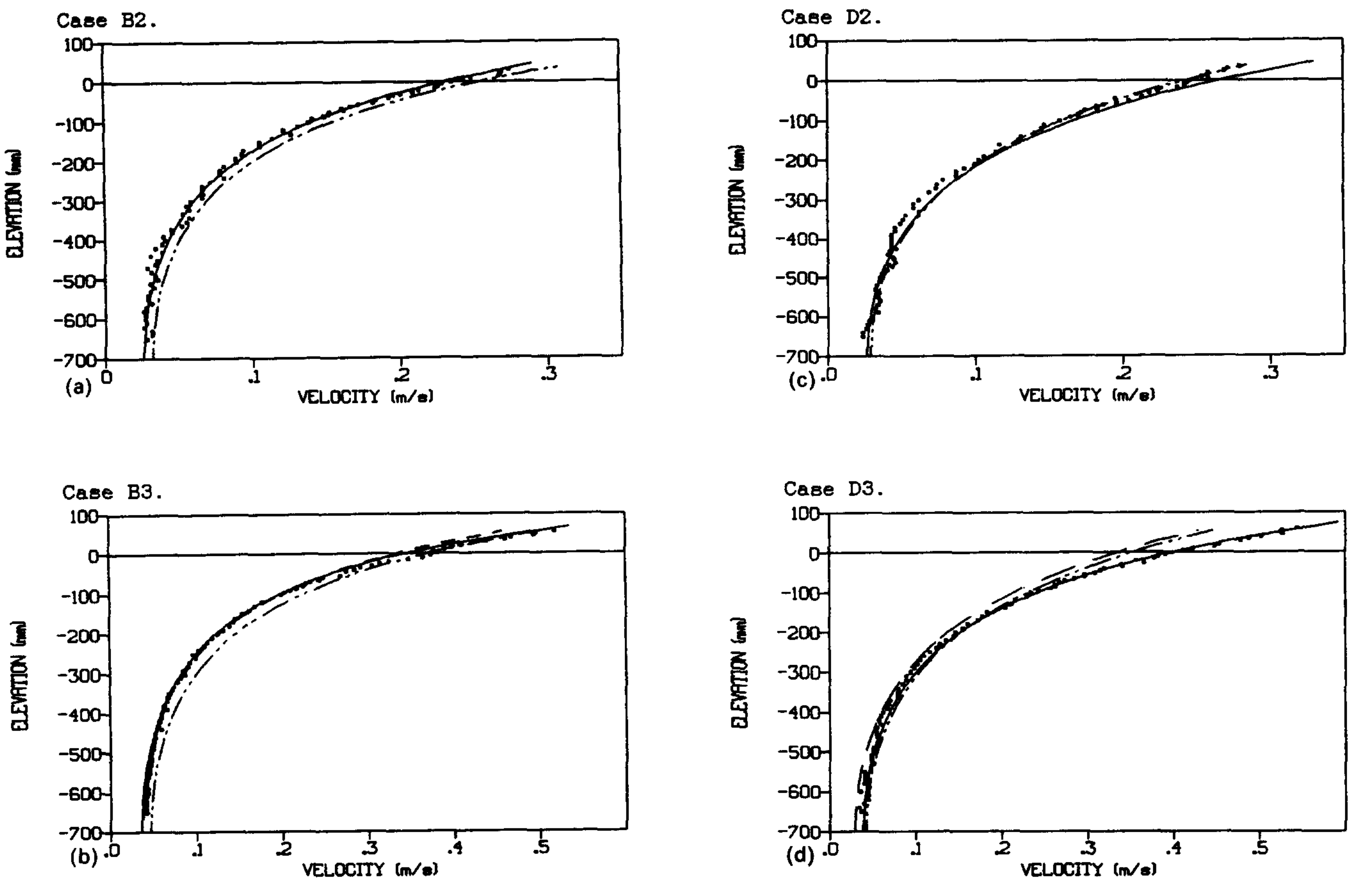

Fig. 5. Peak horizontal velocity, $u(z)$: (■■■) Measured data; (- — -) linear solution; (- - - -) 2nd order solution; (——) numerical model ((a) & (b) $M = N = 18$, $F = 50$; (c) & (d) $M = N = 15$, $F = 50$).

terms of ω and k) is dependent upon the length of the surface record, the number of spatial and temporal positions (I, J) and the order of the proposed solution (M, N). If the record length defines the fundamental period T_1, the number of points (I) must be chosen so that their spacing in time (Δt) is less than or equal to half the shortest wave period, i.e. $\Delta t \leq T_1/(2M)$. Using a similar approach the separation of the points in space (Δx) is given by $\Delta x \leq L_1/(2N)$ where L_1 is the length of the fundamental harmonic $(2\pi/k_1)$ which is calculated within the iterative solution. Although the order of the numerical scheme is not directly comparable to the order of a Stokes' expansion, it is interesting to note that if a 15th order solution has 15 wave frequencies and 15 wave numbers (i.e. $M = N = 15$) a total of 225 individual harmonics are included. If, in this case, the measured surface profile contains a dominant wave frequency which is approximated by the third harmonic (ω_3, k_3), then a 15th order numerical solution includes frequencies up to five times the frequency of the spectral peak. In this case the numerical model will approximately correspond to a 5th order Stokes' solution. However, if the sea state is highly irregular a comparison of this type cannot be made. The numerical calculations presented in Section 4 require a maximum of 324 individual harmonics ($M = N = 18$). In these cases, involving the most non-linear wave groups, the calculations took approximately two hours on a Silicon Graphics (2000) workstation. Other, lower order, calculations were undertaken on a 486 (33 MHz) PC.

4 COMPARISON WITH EXISTING DATA

Regular waves

To investigate the proposed model we first compared the numerical results with a fifth order Stokes' solution (after Fenton[8]) of a non-linear regular wave train ($ak \approx 0{\cdot}33$). In this case the surface elevation $\eta(t)$ generated by the fifth order solution was used as input to the numerical code, and the underlying kinematics were calculated without further constraint (i.e. no attempt was made to restrict the time dependence of the numerical model). A comparison of both the water surface elevation and the underlying kinematics showed that the numerical predictions were in near perfect agreement with the Stokes' solution. Indeed, the maximum 'errors' in the predicted water surface elevation (η) and the horizontal kinematics (u) were 1·3% and 2%, respectively.

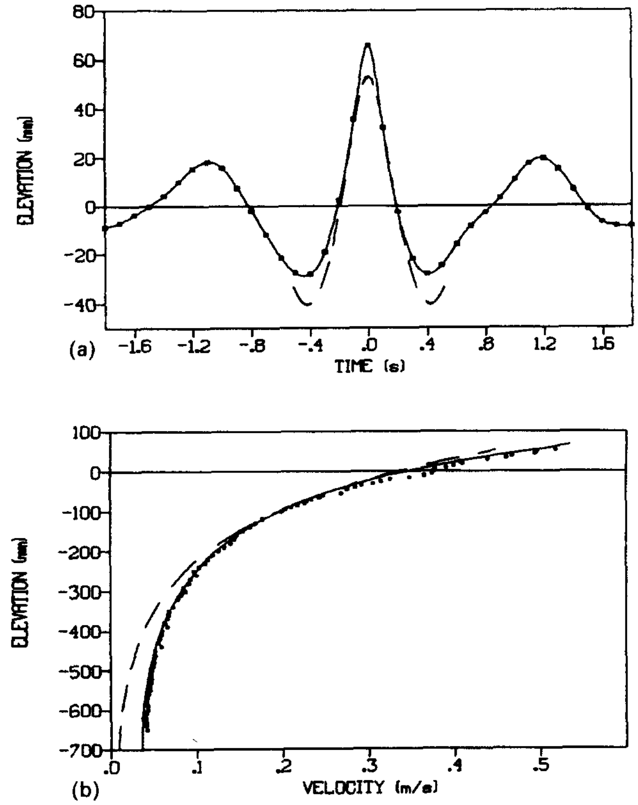

Fig. 6. (a) Surface elevation, $\eta(t)$ at $x = 0$, (b) peak horizontal velocity, $u(z)$. Comparison with 'equivalent' regular wave (Case B3). (▪▪▪) Measured data, (- - - -) fifth order Stokes' solution (after Fenton[8]), (——) numerical solution ($M = N = 18$, $F = 50$).

Transient (time-dependent) waves

In a second (and more testing) investigation the numerical model was compared with the laboratory data presented by Baldock *et al.*[5] This provided experimental measurements of several highly non-linear wave groups. In each case 29 individual frequency components were simultaneously generated by a numerically controlled wave paddle, and the relative phasing of the wave components was adjusted so that constructive interference occurred at one point in space and time. This approach, which was also adopted by Rapp and Melville,[29] produced a large transient wave similar to the 'new wave' formulations presented by Tromans *et al.*[4] The present study will consider two specific data sets (originally referred to as cases B and D) in which the individual wave components were of equal amplitude and were equally spaced within the given period range. In each case we shall consider two input amplitudes such that if A represents the linear sum of the individual wave components, we have $A = 38$ mm and $A = 55$ mm. In these cases Baldock *et al.*[5] provide simultaneous measurements of the water surface elevation $\eta(t)$ and the horizontal velocity components $u(t)$ at the focus location. It is this data which will be compared to the numerical model. The test conditions corresponding to these data sets are outlined in Table 2.

If the wave steepness is defined by the product of the input amplitude (A) and the central wave number (k_c), cases B2 and D2 have a steepness of $Ak_c = 0{\cdot}15$ while B3 and D3 correspond to $Ak_c = 0{\cdot}22$. Previous work on the limiting characteristics of focused wave groups (Rapp and Melville[29] and Baldock *et al.*[5]) has shown that the onset of wave breaking occurs at $Ak_c \approx 0{\cdot}24$. This suggests that cases B3 and D3 are within 10% of their limiting linear amplitude (A_{max}), and consequently the central wave crest will be highly non-linear.

Figure 4(a)–(d) concerns the water surface elevations measured at the focus location for the four cases identified in Table 2. If the maximum crest elevation (for a given input amplitude) provides an indication of the non-linearity of the wave group, the narrow banded spectrum (case D) is more non-linear. The first order (or linear) solution given on Fig. 4(a)–(d) is based upon the amplitudes, frequencies, and wave numbers of the freely propagating small amplitude waves generated at the wave paddle. A comparison with the measured data suggests that a highly non-linear transient wave is characterised by a central wave crest which is higher and narrower than that predicted by a linear sum of the wave components, while the adjacent wave troughs are broader and less deep. The second order solution, based upon the sum of the wave–wave interactions identified by Longuet-Higgins and Stewart,[10] provides an improved description of the water surface elevation. However, the non-linearity of the central wave crest is again underestimated. The experimental data are consistent with the transfer of wave energy into high frequency components which are associated with the higher order wave–wave interactions. A detailed discussion of these points is provided by Baldock *et al.*[5] Figure 4(a)–(d) demonstrates that while a first or second order solution cannot provide an adequate description of the water surface elevation, the proposed numerical scheme is capable of closely approximating the measured wave profile. This is, of course, essential if the underlying kinematics are to be accurately predicted.

The horizontal velocity occurring directly beneath the focused wave crest is shown in Fig. 5(a)–(d). The four cases described in Table 2 are considered and the measured data compared with a linear solution, a second order solution and the present numerical model. The experimental data suggest that the non-linear wave–wave interactions significantly increase the near surface velocities. This is particularly evident in Fig. 5(d) which corresponds to the most non-linear wave group. Furthermore, the gradient of the horizontal velocity with depth ($\partial u/\partial z$ as $z \to \eta$) is larger than that predicted by either a first or a second order solution. At greater depths beneath the water surface ($z \leq d/2$) the linear solution over-estimates the horizontal kinematics. This apparent velocity reduction should not (however) be confused with the second order return flow which arises beneath a regular wave train. Indeed, these

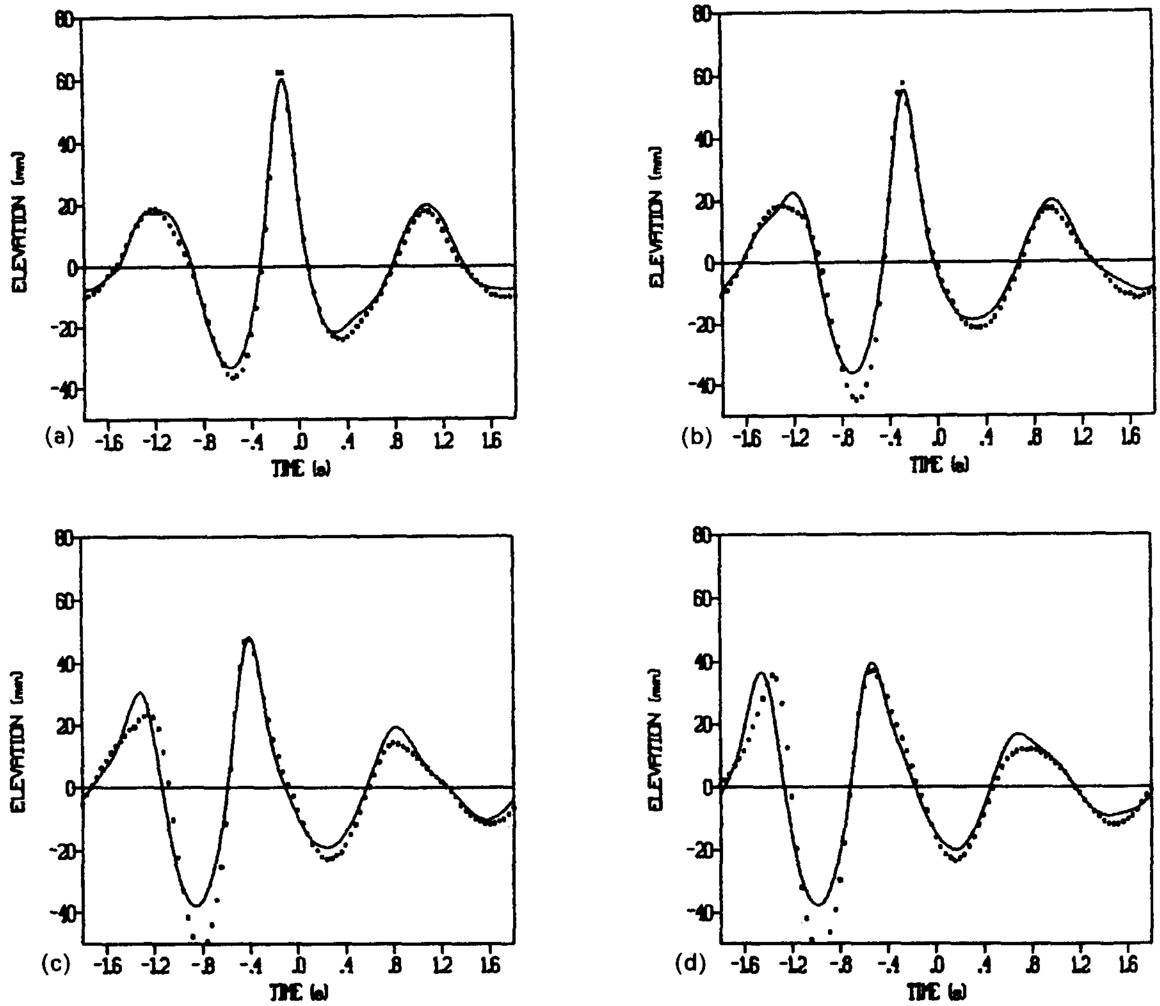

Fig. 7. The spatial evolution of the wave group (Case B3): (· · ·) Measured data; (——) numerical solution ($M = N = 18$, $F = 50$). (a) $x = -0{\cdot}18$ m; (b) $x = -0{\cdot}36$ m; (c) $x = -0{\cdot}54$ m; (d) $x = -0{\cdot}72$ m.

observations are all consistent with the redistribution of wave energy, since the higher frequency components produce large near surface flows which decay rapidly with depth. In contrast to the first and second order solutions, the proposed numerical model provides a good description of the measured data. In particular, the number of frequency components required to model both the water surface elevation and the underlying kinematics increases with the amplitude of the wave group. This is consistent with the normalised power spectra provided by Baldock *et al.*[5] Furthermore, the fundamental wave number increases with the amplitude of the wave group, thereby implying an overall steepening of the wave envelope.

To emphasise the importance of the time dependent terms within a focused wave group Fig. 6(a) & (b) compare the broad banded case (B3) with a higher order Stokes' solution (Fenton[8]). In this comparison an 'equivalent' wave period was estimated from the zero crossing points measured at the focus location, and the wave height (H) was determined from the measured data. Figure 6(a) compares the measured and predicted water surface elevation and shows that a regular wave solution does not provide a good representation of a large transient wave. In particular, the Stokes' solution under-estimates the maximum crest elevation by approximately 20%. This comparison highlights the increased crest–trough asymmetry which occurs within a focused wave group. This has important implications for the calculation of air gaps. Figure 6(b) concerns the horizontal velocity measured directly beneath the focused wave crest. In this case the Stokes' solution under-estimates the kinematics at all depths. These results suggest that both the total base shear and the over-turning moment will be significantly under-estimated by a steady solution based upon an 'equivalent' regular wave.

Although the maximum crest elevation (producing the most extreme kinematics) is of primary importance for design calculations, the present solution may also describe the flow field at other spatial locations. Figures 7(a)–(d) and 8(a)–(d) compare the measured and predicted surface elevations, $\eta(t)$, for cases B3 and D3 at four spatial locations in the vicinity of the focal point

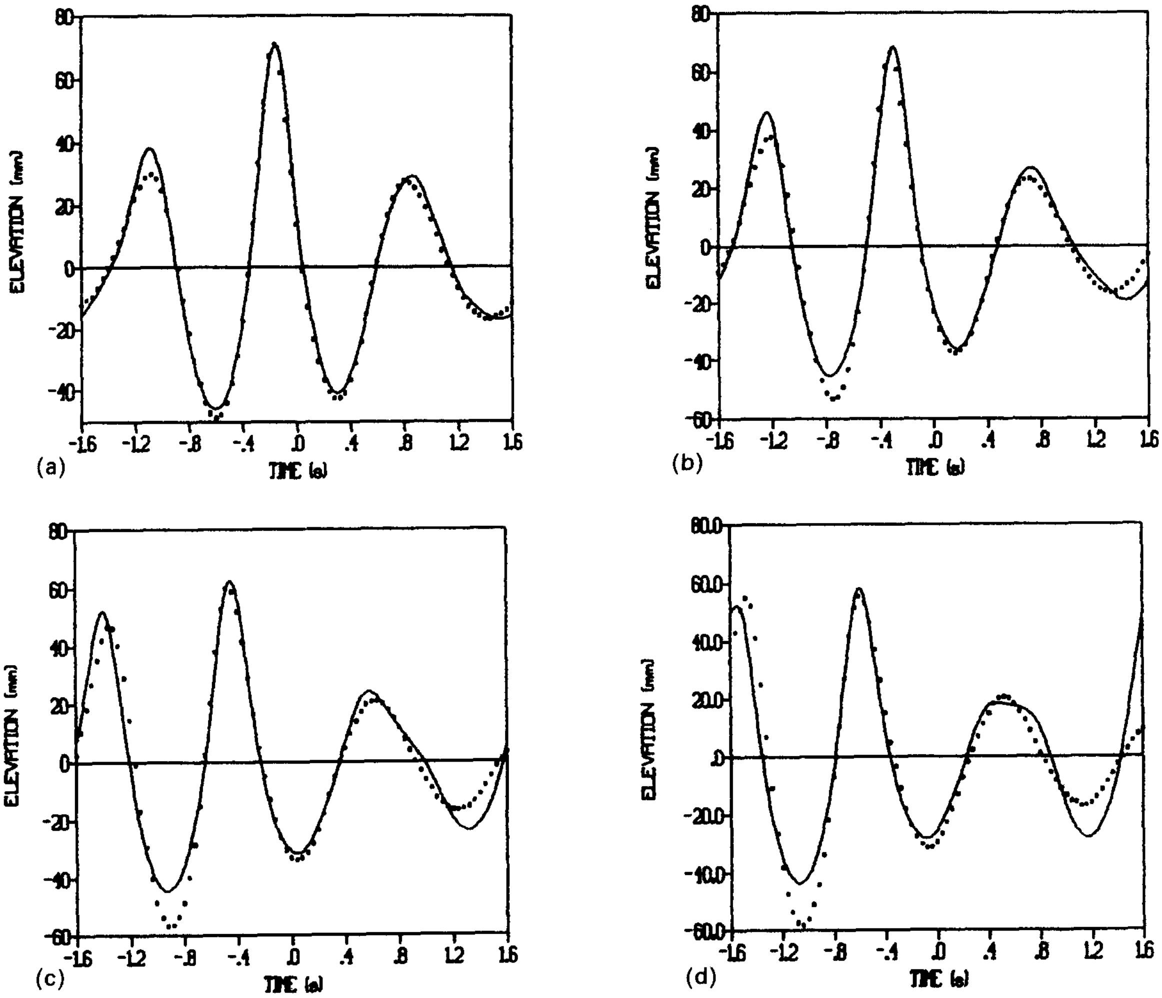

Fig. 8. Spatial evolution of the wave group (Case D3): (···) Measured data; (——) numerical solution ($M = N = 15$, $F = 50$). (a) $x = -0{\cdot}22$ m; (b) $x = -0{\cdot}44$ m; (c) $x = -0{\cdot}66$ m; (d) $x = -0{\cdot}88$ m.

($x = 0$). In each case the predicted water surface elevation is in reasonable agreement with the measured data. Indeed, this agreement is perhaps better than one might expect given that the input to the numerical model merely corresponds to the time series at one spatial location ($x = 0$). These results suggest that the Fourier series given in eqn (6), together with the error minimisation outlined in eqns (8)–(15), provides a reasonable description of the wave components arising within a highly non-linear random sea state.

Figures 7(a)–(d) and 8(a)–(d) also suggest that the 'errors' in the predicted water surface elevation are dependent upon the distance from the input data (at $x = 0$), and primarily arise near the boundaries of the time domain (i.e. $t \approx \pm 1{\cdot}6$ s). This is particularly apparent in Fig. 8(d) (case D3 at $x = -0{\cdot}88$ m) where the description of the surface profile for $|t| \geq 1{\cdot}0$ s is poor. The 'errors' within this region arise because the numerical model is based upon a fundamental harmonic (in this case $T_1 = 3{\cdot}2$ s) and therefore assumes that although the surface profile deforms within this domain, $\eta\,(x = -0{\cdot}88,\ t = -1{\cdot}6) = \eta\,(x = -0{\cdot}88,\ t = +1{\cdot}6)$. This assumption is incorrect and significant errors will result if a large wave occurs at one end of the time domain. This situation arises in Fig. 8(d) and consequently the waves at $t \approx \pm 1{\cdot}2$ s are inadequately modelled. Difficulties of this type may, however, be overcome by increasing the fundamental period and including more Fourier components. Unfortunately, this also increases the computational effort required for convergence.

5 CONCLUSIONS

The present paper has considered the description of a two dimensional non-linear wave group generated by the focusing of wave components within a random sea state. A numerical model based upon a Fourier series expansion in space and time has been described, and the results compared to recent laboratory data presented by Baldock *et al.*[5] This comparison suggests that if the time history of the water surface elevation is known, or can be predicted from the statistical characteristics of the sea state (Tromans *et al.*[4]), the numerical model will provide a good fit to both the measured water surface elevation and the underlying kinematics. In particular, the proposed solution can incorporate a large number of frequency components with a wide range of phase velocities. This enables the solution to define the appropriate mix of free waves and their associated bound waves which minimise the error in the non-linear free surface boundary conditions. As a result, the proposed solution is capable of modelling the high frequency waves which are generated by the non-linear wave–wave interactions. It is these components which produce both the large water surface elevations at the focus position and the increased kinematics near the water surface.

Further comparisons with the laboratory data suggest that while the present numerical model provides a good description of the focused wave groups, a steady wave solution based upon an 'equivalent' regular wave does not. In particular, a higher order Stokes' solution will under-estimate both the maximum crest elevation (for a given wave height) and the magnitude of the horizontal velocity. The numerical model is also able to predict the time history of the water surface elevation away from the focus position. In these cases the numerical predictions are in reasonable agreement with the laboratory data provided that the fundamental period is of sufficient duration to negate the periodic constraint, and the number of Fourier components is sufficiently large to provide the required resolution.

In a real three dimensional sea the focusing of wave energy to produce a large transient wave will incorporate both directional and frequency spreading. Although the proposed model cannot (at present) rigorously define the non-linear interactions within a short-crested sea, the effect of directional spreading may be at least partially included by applying a pre-determined spreading function to the calculated kinematics. The proposed model is based upon a simple numerical procedure which is not computationally intensive. Furthermore, the solution is robust in the sense that convergence was achieved in all cases with simple initial conditions. We therefore conclude that the present model is appropriate for design calculations where a description of the water surface elevation is available (or can be calculated), but the underlying kinematics are unknown.

ACKNOWLEDGMENTS

The authors gratefully acknowledge the financial support provided by the Science and Engineering Research Council (SERC), The Royal Society (under the Research Grants Scheme) and Shell UK, Exploration and Production.

REFERENCES

1. Dean, R. G. Stream function representation of non-linear ocean waves. *J. Geophys. Res.*, **70** (18) (1965) 4561–72.
2. Rozario, J. B., Tromans, P. S., Taylor, P. H. & Efthymiou, M. Comparisons of loads predicted using 'New Wave' and other wave models with measurements on the Tern structure. In *Wave Kinematics and Environmental Forces*, **29**, SUT. Kluwer, 1993, pp. 143–58.
3. Sand, S. E., Otessen Hansen, N. E., Klinting, P., Gudmestad, O. T. & Sterndorf, M. J. Freak wave kinematics. In *Water Wave Kinematics*, eds Torum & Gudmestad, NATO ASI Ser. 1990, pp. 535–48.
4. Tromans, P. S., Anaturk, A. & Hagemeijer, P. A new model for the kinematics of large ocean waves — application as a design wave. *Proc. 1st Int. Conf. Offshore and Polar Engineering*, **3**, Edinburgh, 1991, pp. 64–71.
5. Baldock, T. E., Swan, C. & Taylor, P. H. An experimental investigation of 2-D wave groups. *Phil. Trans. Roy. Soc.*, (1994) (submitted).
6. Tromans, P. S., Efthymiou, M., van der Graaf, J. W., Vanderschuren, L. & Taylor, P. H. Extreme storm loading on fixed offshore structures. *Proc. 6th Int. Conf. on the Behaviour of Offshore Structures (BOSS)*, **1**, London, 1992, pp. 325–36.
7. Lambrakos, K. F. Extended velocity potential wave kinematics. *J. Waterways Port Coastal & Ocean Engng.*, **107** (1981) 159–74.
8. Fenton, J. D. A fifth order Stokes' theory for steady waves. *J. Waterways Port Coastal & Ocean Engng.*, **111** (1985) 216–34.
9. Kinsman, B. *Wind Waves*. Dover, New York, 1965.
10. Longuet-Higgins, M. S. & Stewart, R. W. Changes in the form of short gravity waves on long waves and tidal currents. *J. Fluid Mech.*, **8** (1960) 565–83.
11. Longuet-Higgins, M. S. The propagation of short surface waves on longer gravity waves. *J. Fluid Mech.*, **177** (1987) 293–306.
12. Dean, R. G. Freak waves: A possible explanation. In *Water Wave Kinematics*, eds Torum & Gudmestad, NATO ASI Ser, 1990, 609–12.
13. Petti, M. On the separation of second order components for non-linear wave spectra. In *Computer Modelling in Ocean Engineering 91*, eds Arcilla *et al.*, Balkema, Rotterdam, 1991, pp. 201–8.
14. Forristall, G. Z. Irregular wave kinematics from a kinematic boundary condition fit. *Appl. Ocean Res.*, **7** (1985) 202–12.
15. Sobey, R. J. Wave theory predictions of crest kinematics. In *Water Wave Kinematics*, eds Torum & Gudmestad, NATO ASI Ser, 1990, pp. 215–31.
16. Wheeler, J. D. Method for calculating forces produced by irregular waves. *Proc. 1st Annual Offshore Technology Conf.* Houston, **1**, 1970, pp. 71–82.
17. Chakrabarti, S. K. Discussion on dynamics of single point mooring in deep water. *J. Waterways, Harbours and Coastal Eng. Div.*, ASCE, **97** (1971) 588–90.
18. Rodenbusch, G. & Forristall, G. Z. An empirical method for random directional wave kinematics near the free surface. *Proc. 18th Annual Offshore Technology Conference*, OTC 5097, Houston, 1986.
19. Lo, J. & Dean, R. G. Evaluation of a modified stretched linear wave theory. *Proc. 20th Int. Conf. on Coastal Engineering*, ASCE, **1**, 1986, pp. 522–36.
20. Gudmestad, O. T. & Connor, J. J. Engineering approximation to non-linear deep water waves. *Appl. Ocean Res.*, **8** (1986) 76–88.
21. Gudmestad, O. T. & Haver, S. Uncertainties in the prediction of wave kinematics in irregular waves. In *Wave Kinematics and Environmental Forces*, **29**, SUT. Kluwer, 1993, pp. 75–100.
22. Dold, J. W. & Peregrine, D. H. Steep unsteady waves: An

efficient computational scheme. *Proc. 19th Int. Conf. on Coastal Engineering*, ASCE, **1**, 1984, pp. 955–67.
23. Skyner, D. J., Gray, C. & Greated, C. A. A comparison of time-stepping numerical predictions with whole-field flow measurement in breaking waves. In *Water Wave Kinematics*, eds Torum & Gudmestad, NATO ASI Ser, 1990, pp. 491–508.
24. Sobey, R. J. A local Fourier approximation method for irregular wave kinematics. *Appl. Ocean Res.*, **14** (1992) 93–105.
25. Fenton, J. D. Polynomial approximations and water waves. *Proc. 20th Int. Conf. on Coastal Engineering*, ASCE, **1**, 1992, pp. 193–207.
26. Chappelear, J. E. Direct numerical calculation of wave properties. *J. Geophys. Res.*, **66**(2) (1961) 501–8.
27. Chaplin, J. R. Developments of stream-function wave theory. *Coastal Engineering*, **3** (1980) 179–205.
28. Press, W. H., Flannery, B. P., Teukolsky, S. A. & Vetterling, W. T. *Numerical Recipes*. Cambridge University Press, 1989.
29. Rapp, R. J. & Melville, W. K. Laboratory measurements of deep water breaking waves. *Phil. Trans. Royal Soc.*, **A331**, 1990, pp. 735–800.